Journal of Soil Science and Plant Nutrition
https://doi.org/10.1007/s42729-023-01373-6

ORIGINAL PAPER

Linear Macropore Installation to Reduce Red-Soil Erosion in Sugarcane Fields

Eisei Morioka[1] · Thanh Long Bui[1] · Yasushi Mori[1] · Kazutoshi Osawa[2] · Akira Hoshikawa[3]

Received: 30 August 2022 / Accepted: 23 June 2023

Abstract
This study determines the cause of soil erosion in red soils in sugarcane fields, especially even with the use of subsoiling fissures, and to compare the effectiveness of a novel artificial linear-macropore with the insertion of fibrous material into the fractures. Four column treatments (tillage, subsoiling, linear-macropore with plant residue fillings, and no-tillage-with-mulching) were established. A subsoiler was used to break up hard soil layers to enhance infiltration, whereas mulching reduced the impact of raindrops on the soil. Sugarcane residue was inserted in the empty fissure to reinforce the structure, making linear macropore. Simulated rainfall with 20 mmh^{-1} was applied to the soil surface for 6 h per day for two days. Surface runoff, soil erosion, and drainage were measured during each run. Erosion was minimal (1/7 reduction), and bottom drainage was observed in the linear-macropore and no-tillage-with-mulching plots. Conversely, due to the formation of an impermeable layer or surface crust, high erosion (0.282 t-C ha^{-1} yr^{-1}) and decreased drainage levels were detected in the subsoiling and tillage plots. Moreover, the aboveground protrusion of fibrous material at the linear-macropore maintained infiltration, even following crust formation. Field application of these four management strategies revealed the effectiveness of linear-macropore and mulching in reducing surface flow. Linear-macropore application maintains appropriate levels of infiltration, and insertion of plant residue fillings reinforces the macropore structure while also avoiding clogging. Hence, the linear-macropore scheme may represent an effective strategy for reducing surface runoff and red soil erosion.

Keywords Soil erosion · Surface runoff · Macropore · No-tillage · Sugarcane

1 Introduction

In the Okinawa region of Japan, which is located in the subtropical zone, red soil runoff causes loss of nutrient-rich topsoil, leading to reduced agricultural productivity. Agricultural surface soils contain a large amount of organic matter, while soil erosion, which occurs with surface flow, also significantly disrupts the terrestrial carbon budget (Wang et al. 2017). In addition, tropical soils are inherently vulnerable to organic matter loss due to rapid weathering and thin organic matter layers caused by intense solar radiation and poor land management (Guillaume et al. 2015). Under these conditions, the impact of soil erosion due to heavy rainfall is likely significant (Lal 2001). The eroded topsoil is then transported into the ocean, adversely affecting coral reef ecosystems, which require clear, nutrient-poor waters to grow (Ikeda and Kan 2014). Agricultural land is responsible for most of the erosion of red soil (Nakasone et al. 1998). During the early stages of cropping, a significant proportion of agricultural land is bare, thus highlighting the need for improved measures to reduce surface runoff and soil erosion.

There are several measures that can be taken to prevent soil erosion as part of agricultural practices. For instance, mulching with sugarcane residue and no-till farming effectively reduce red soil erosion (Noda et al. 2009; Osawa et al. 2005; Tebrügge and Düring 1999). In no-till farming, sugarcane residue acts as a mulch to mitigate the effects of raindrops, thereby preventing red soil erosion. In fact, no-till cultivation techniques are becoming increasingly popular globally, as means to reduce soil movement toward

✉ Yasushi Mori
yasushim@cc.okayama-u.ac.jp

[1] Graduate School of Environmental and Life Science, Okayama University, 3-1-1 Tsushimanaka, Okayama 700-8530, Japan

[2] School of Agriculture, Utsunomiya University, 350 Minemachi, Utsunomiya 321-8505, Japan

[3] Sekiseishouko Coral Reef Fund, 221 Ishigaki, Ishigaki 907-0023, Japan

Published online: 05 July 2023

lower elevation (Komissarov and Klik 2020), reduce soil compaction by heavy machinery (Richard et al. 2001), reduce global warming (Yagioka et al. 2015), and increase biological diversity (Miura et al. 2016). In contrast, tilling destroys soil aggregates, increases contact with oxygen, and tends to accelerate organic matter decomposition (Six et al. 2000). Although the application of no-tillage has gradually increased within the Okinawa region, yields have continued to decrease in semi-humid and humid areas (Kanazawa 1995). Moreover, the aversion of farmers to landscapes with plant residues and weeds has limited the application of no-till farming.

To avoid soil erosion while mitigating the current reduction in revenue and landscape degradation, the primary research focus has shifted toward investigating subsoil crushing management, which can be accomplished with machinery and does not negatively impact the landscape. More specifically, this strategy improves permeability by crushing hard soil layers to create fissure-like gaps and is a management technique described in the sugarcane cultivation guidelines (Okinawa Prefecture 2014). However, it is unclear how long this technique, developed in the temperate zones, will remain effective when exposed to the heavy rainfall unique to subtropical regions. In particular, within the subtropical climate of the Okinawa region, subsoiler treatments that create vertical fissures may initially prove effective; however, the intense rainfall and the typhoons passing through the subtropical zone may ultimately cause erosion, resulting in small particles clogging subsoil cracks. Accordingly, we have adopted an artificial macropore system to address red soil erosion.

Artificial macropores are constructed to mimic the structural characteristics of root pores in natural soils (Mori et al. 1999a, b) while also promoting vertical infiltration and horizontal diffusion (Mori and Higashi 2009; Mori et al. 2013). Solute transport through artificial macropores has been investigated numerically (Lamy et al. 2009) and experimentally (Gjettermann et al. 2004), and this preferential flow enhanced salt leaching in the arid area (Zhang et al. 2021).

In previous studies, artificial macropores—cylindrical pores filled with fibrous material—were introduced to the soil (Mori and Hirai 2014; Mori et al. 2014). As empty macropores are prone to collapse and clogging, fibrous materials are inserted to reinforce the structure and induce water flow through capillary forces (Mori and Hirai 2014). Application of this process has successfully enhanced infiltration, increased the soil organic matter content, and nearly doubled plant biomass production at a faster rate than expected (Mori et al. 2014).

Therefore, in the current study, we describe a novel artificial macropore design based on the insertion of fibrous material into a subsoiling gap. As this strategy represents the linear form of a cylindrical artificial macropore, we have designated it *linear macropore*. The fibrous material used was sugarcane leaf residue (locally available and easily accessible) from agricultural land. The primary objective of this research was to evaluate soil surface management, namely, tillage, subsoiling, no-tillage-with-mulching, and a linear-artificial-macropore, to reduce surface runoff and red soil erosion. Simulated rainfall was applied to observe surface runoff and sediment loss. Moreover, a 2D numerical simulation was conducted to assess surface flow and infiltration.

2 Materials and Methods

2.1 Examined Soils

A soil prone to erosion was sampled from a sugarcane field (24°21′56" N, 124°07′34" E) located in the southwestern region of Ishigakijima Island, Okinawa, Japan. The mean annual temperature and precipitation from 1981 to 2010 were 24.3 °C and 2106.8 mm, respectively (Japan Meteorological Agency 2023). Soils were Kunigami Mahji (Onaga and Gibo 1984), or Haplic Acrisols (Chromic) (World Reference Base for Soil Resources 2006). The sugarcane field was ~ 80 m long and sloped 3% from west to east, which is the standard on Ishigakijima Island.

The characteristics of this soil are listed in Table 1. The hydraulic conductivity at 0–10 cm depth measured with the core sample was 3.16×10^{-4} cm s^{-1}. The sample column was filled with soil samples that were passed through a 2-mm sieve at a dry density of 1.20 Mg m^{-3} and with an initial volumetric water content of 0.15 m^3 m^{-3} to match the field conditions.

Table 1 Characteristics of examined soil

	depth (cm)		
	0 cm	10 cm	30 cm
Sand	38.22(7.30)	28.53(7.51)	23.97(4.33)
Silt	40.35(3.07)	47.27(7.23)	48.05(4.37)
Clay	21.43(4.90)	24.2(0.30)	27.98(2.33)
TC(%)	1.73(0.93)	1.10(0.19)	0.91(0.02)
TN(%)	0.172(0.111)	0.115(0.004)	0.113(0.006)
K(mg 100 g^{-1})	27.2(7.1)	19.2(6.1)	15.1(3.9)
P(mg 100 g^{-1})	3.70(2.95)	1.15(0.66)	1.05(0.40)
Mg(mg 100 g^{-1})	25.5(14.7)	20.6(3.0)	17.4(1.3)
Fe(mg kg^{-1})	0.407(0.155)	0.329(0.004)	0.272(0.017)

The numbers in parentheses show standard deviations

2.2 Column Setup

Figure 1 shows a schematic of our experimental apparatus. Acrylic columns (inner diameter 4.9 cm, height 10 cm) were used in the setup. A small hole (inner diameter: 1 cm) was made immediately beside the soil surface to collect surface water. When the rainfall intensity exceeded the infiltration capacity of the soil, the surface layer became slightly flooded and tiny pools of water appeared. Once flooding occurred, surface runoff water was captured, as shown in Fig. 1. For effluent sampling, rectification plates with multiple holes (0.2 cm diameter) and a nylon mesh were placed at the bottom of the column to prevent soil particle loss while collecting the effluent.

The surface runoff and downward drainage water were measured with an electronic balance connected to a PC and recorded at 5-min intervals. The sampled surface water containing sediment was oven-dried at 105 °C, and the amount of sediment discharge was measured.

2.3 Simulated Field Management

We simulated four types of sugarcane cultivation management schemes (Fig. 1), namely, (1) tillage, (2) tillage plus subsoil treatment (empty fissure), (3) tillage plus subsoil treatment with sugarcane leaf residue (linear macropore), and (4) no-tillage with mulching. In the tillage plot, the soil surface was lightly scratched after repacking. In the no-tillage plot, air-dried sugarcane residue from the field was spread evenly over the soil surface, as no-tillage management often includes the distribution of intact plant residues in the field. For the subsoiling treatment, after repacking the soil, fissures (4.9 cm long, 0.5 cm wide, and 5 cm deep) were cut with a soil knife (Fig. 1). Moreover, for the linear-macropore treatment (Fig. 1), we inserted sugarcane leaf residue into the fissures at a density of ~ 0.1 Mg m^{-3}. The sugarcane leaf residue was placed such that the "heads" protruded above the soil surface to prevent clogging under flooding conditions (Mori et al. 2014).

2.4 Simulated Rainfall

Given that the impact of raindrops during heavy rain is a vital factor to consider when simulating surface management effects, we developed a rainfall device that "drips" water droplets randomly and equally across the soil surface by four needles. Droplet release was controlled by the pressure from a pump, gravity, and friction at the inner wall of the release needle. Here, the friction should be sufficient to resist gravity. Otherwise, the release would be primarily controlled by gravity, preventing a consistent rainfall between the four needles and spatial distribution on the soil surface. Five needle types (18, 20, 22, 27, and 30 G) were tested in the device (Fig. 1), and preliminary rainfall experiments were conducted at a rainfall intensity of 20 mm h^{-1}. The data fluctuation, i.e., the coefficient of variation (CV), was affected by the inner diameter of the needles (Table 2). As the 27 G needle (inner diameter 0.2 mm, outer diameter 0.41 mm, and length 12.7 mm; DPN-27G-1, Musashi Eng. Co. Ltd., Tokyo) exhibited the smallest fluctuation, it was selected for further experimental use. The pump feeding rate was adjusted for the 27 G needle to apply 20 mm h^{-1} of rainfall.

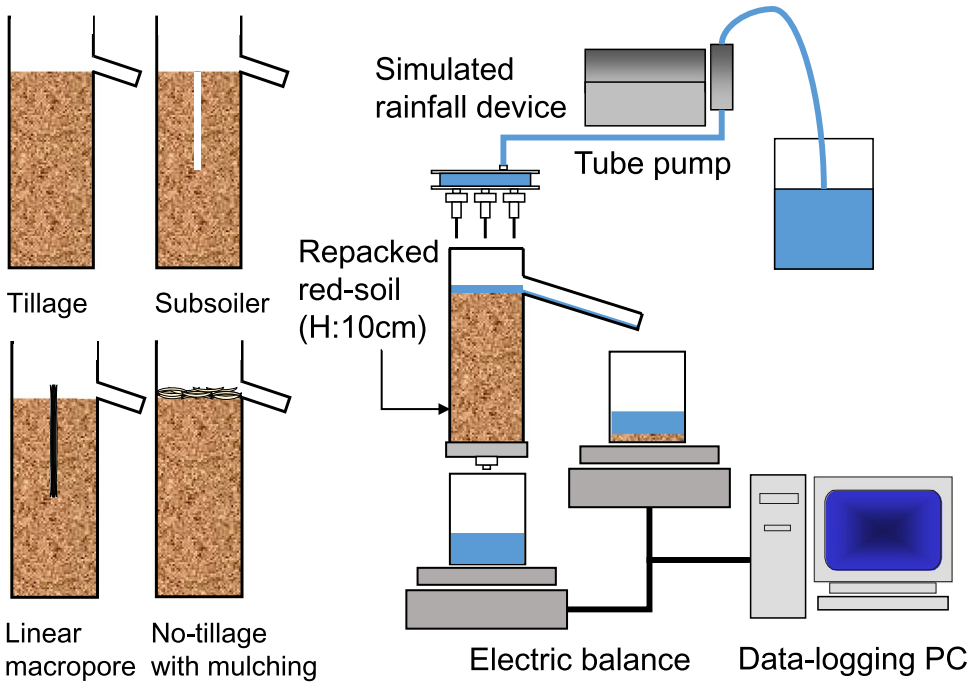

Fig. 1 Schematic diagram of the experiment. Four types management were employed, that were (1) tillage, (2) subsoiler (empty fissure, width 5 mm depth 50 mm), (3) subsoiler with sugarcane leaf residue inserted (linear macropore), and (4) no-tillage with mulching

Table 2 Selection of needle gauge for simulated rainfall

Gauge size (unit)	O.D. mm	I.D. mm	Average mm/h	S.D. mm/h	C.V.
18G	1.27	0.84	5.52	7.48	1.36
20G	0.91	0.58	5.43	4.21	0.78
22G	0.71	0.41	5.25	1.93	0.37
27G	0.41	0.20	4.64	0.16	0.03
30G	0.31	0.13	5.58	0.27	0.05

20 mm h^{-1} of rainfall was applied, and 5 mm h^{-1} was expected for each needle

The rainfall device was mounted 3.3 cm above the soil surface, and rainfall was produced via a microtube pump (PSM 050DA, Advantec, Tokyo) with 2 × 4-mm silicon tubes (AS-ONE Corporation, Osaka). The simulated rainfall was applied for 6 h at an intensity of 20 mm h^{-1} (total amount 225 mL) to match the local conditions. We selected 20 mm h^{-1} as strong rainfall (Japan Meteorological Agency 2023), lower than the 25 mm h^{-1} reported by Hudson (1981), to observe the initial runoff and erosion under typhoon or heavy rain conditions that could cause soil erosion. The simulated rain was reapplied under the same conditions 24 h after the end of the first rainfall period, as natural rain occurs intermittently. The experiment (two simulated rainfall periods) was repeated three times for each type of soil surface management.

2.5 Two-dimensional Numerical Simulation of Water Flow

The infiltration process in the sample columns was simulated using the HYDRUS (2D/3D) software (PC-PROGRESS, Prague, Czech Republic), which can simulate water and solute transport in variably saturated soils (Simunek et al. 2007). Calculations were performed for the four soil management methods. The same rainfall intensity of 20 mm h^{-1} as in the column experiment was used for the two-dimensional simulations.

The calculation domains with and without macropores were set to observe different surface runoff and downward movements caused by the different soil surface treatments. We also simulated conditions with/without a surface crust, as a surface crust, or impermeable layer, may form on the soil surface when erosive soils are exposed to rain drop impact. In addition, we assessed the mulching effect by applying a 5-mm plant residue layer on the soil surface. The van Genuchten parameters (van Genuchten 1980; Mualem 1976) used in the calculation domain are listed in Table 3.

2.6 Preliminary Farming using the Four Treatments

The goal of this study was to develop a soil erosion control strategy that farmers can implement. Experiments on a small scale were conducted first, as these treatments, if applied in a farmer's field without evaluation, could affect the entire sugarcane crop and the surrounding water environment during the crop season to the detriment of the farmer. Therefore, after obtaining initial data and confirming the validity of the experiment, the same four treatments were applied on the actual farm with the farmer's permission to ensure the representativeness of this experimental setup. The depth and width of the fissures were 25 and 5 cm, respectively, and sugarcane leaves were inserted at a density of 0.1 m^3m^{-3}.

3 Results

3.1 Surface Runoff and Infiltration/Drainage

During the first rainfall period from 0–60 min, most rainfall infiltrated into the soil, and surface runoff water was rarely observed in any treatment (Fig. 2a). After 60 min, surface runoff water gradually became noticeable in the tillage and subsoil treatments, with significant surface runoff detected in the latter. By the end of the first rainfall period, approximately half of the rainfall flowed from the surface. Surface runoff began in the linear-macropore and no-tillage-with-mulching treatments 130 min after rainfall initiation. The cumulative surface runoff water at the end of the first rainfall period was ~ 15–20% of the applied rainfall volume.

During the second rainfall period (Fig. 2b), the largest amount of surface runoff water was observed in the subsoil treatment (~ 86%), followed by the tillage, no-tillage-with-mulching, and linear-macropore treatments (~ 70% each; Fig. 2b). Moreover, during the second rainfall period, the time at which surface runoff became apparent differed

Table 3 van Genuchten parameters for 2D simulation

	θr	θs	α	n	$Ks\ (mm\ h^{-1})$	l
Red soil	0.050	0.448	0.015	1.233	13.96	0.5
Air	0.001	1	24	3	9936	–3
Macropore	0.037	0.832	0.154	2.103	92880	0.5
Crust	0.086	0.38	0.0008	1.09	0.5	0.5
Plant residue	0.045	0.430	0.145	2.68	297	0.5

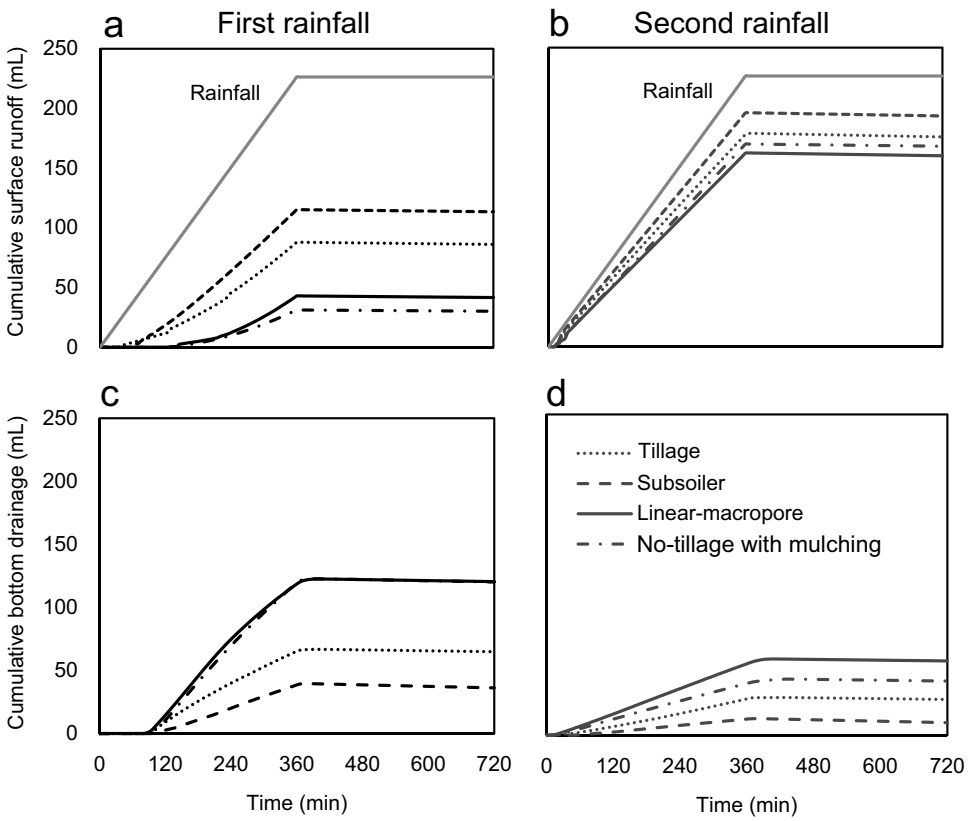

Fig. 2 Change in surface runoff water and drainage water during the first and second rainfall periods. **a** and **b** denote surface runoff; **c** and **d** denote bottom drainage; average data for three repetitions are shown

significantly from that of the first rainfall period. That is, surface runoff was generated in all treatments within 15–20 min of rainfall initiation. The cumulative surface runoff water increased significantly for all treatments relative to the first rainfall period, as the soil was relatively saturated at the initiation of the second rainfall period.

Additionally, within the first 90 min of the first rainfall period, drainage water was detected in all treatments at the bottom of the samples (Fig. 2c). Although the average cumulative drainage amount differed among treatments, that for the linear-macropore and no-tillage-with-mulching treatments was similar (~ 50%), while that in the tillage and subsoil treatments was ~ 25 and 15% of the applied rainfall, respectively.

During the second rainfall period (Fig. 2d), the cumulative drainage water volume was the highest in the linear-macropore treatment, followed by the no-tillage-with-mulching, tillage, and subsoil treatments. Similarly, the ratio of discharged water volume to simulated rainfall was the largest in the linear-macropore treatment (26%) and the smallest in the subsoil treatment (4%). Moreover, relative to the first rainfall period, drainage water was detected earlier during the second rainfall period. We estimated that the soil was close to saturation 24 h after the first rainfall period, as gravity drainage rarely occurs in soil with high clay content. In the linear-macropore and no-tillage treatments, drainage was observed 15–20 min after the second rainfall initiation, whereas in the tillage and subsoil treatments, it was observed within ~ 30 and 50 min following rainfall initiation, respectively. Here, we noted that a smaller amount of drainage corresponded to a reduced infiltration capacity.

3.2 Formation of a Surface Crust

The formation of an impermeable "crust" was detectable on the surface soil in the tillage, subsoiling, and linear-macropore treatments, whereas no crust was visible in the no-tillage-with-mulching treatment (Fig. 3). Surface crusts are formed when raindrops collide with the soil surface, effectively detaching soil particles from the surface, which are carried by moving water, leading to their accumulation and subsequent clogging of pore spaces (Morin et al. 1981; Moss 1991). This process continued throughout the rainfall period, effectively generating a thin yet impermeable layer. However, covering the soil surface with sugarcane leaf residue prevented the formation of a crust in the no-tillage-with-mulching treatment.

In the subsoiling treatment, the pre-generated fissures were blocked, so that they were not visible at the end of the experimental period (Fig. 3b). However, when the column was cut horizontally at the midpoint, the fissures were still present (Fig. 3b'), indicating that only surface level clogging

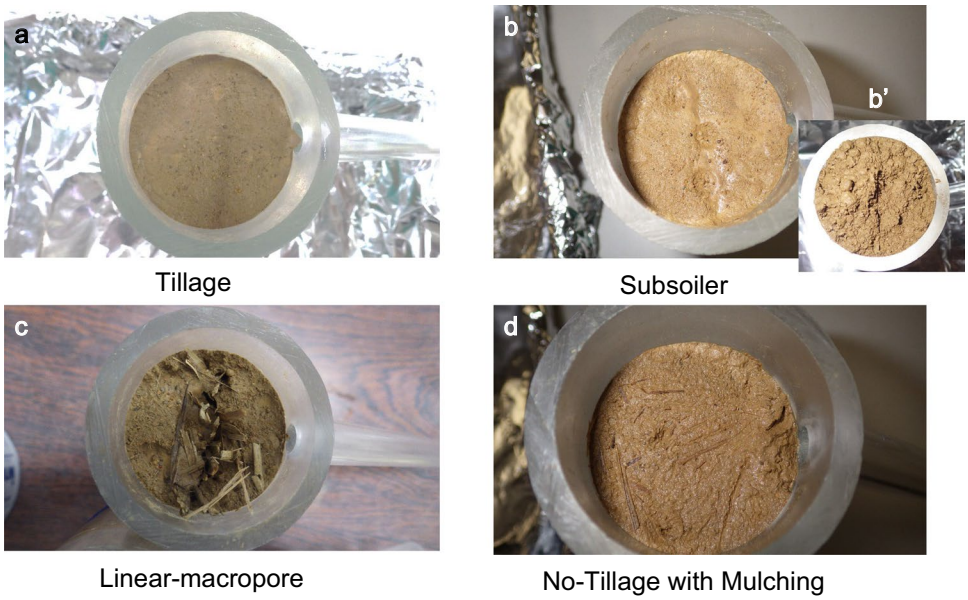

Fig. 3 Soil surface for each treatment after rainfall; (**a**) tillage, (**b**) subsoiler, (**c**) linear-macropore, (**d**) no-tillage-with-mulching. b', fissure appearance at the midpoint of the column, following sealing of the soil surface with small particles

occurred, which is characteristic of thin crust formation at the soil surface.

3.3 Infiltration Process and 2D-simulation

A 2D simulation using Hydrus2D (Fig. 4) revealed differences in infiltration between each treatment after the first hour of rainfall in the presence or absence of crust formation. When no crusts formed, the macropore structure clearly promoted downward infiltration (Fig. 4b). Moreover, the presence of plant residues on the surface not only reduced the impact of raindrops but also promoted downward infiltration by storing water at the soil surface (Fig. 4c), resulting in a superior infiltration as compared to that achieved with tillage (Fig. 4a). These findings are consistent with those of Oka et al. (2022). On the contrary, when surface crusts formed in the top-five millimeters of the surface soil (Fig. 4d, e, f), minimal infiltration was observed in the case of tillage, which is consistent with the large amount of surface flow (Fig. 2). On the contrary, artificial macropores which contained plant residues protruding above the soil (Fig. 1) allowed downward infiltration even in the presence of surface crusts (Fig. 4e). These findings agree with our experimental results (Fig. 2), in which the downward infiltration was equivalent to no tillage. However, subsoiler fissures were readily sealed by small particles (Fig. 3b); thus, despite the existence of macropore structures in the lower part of the topsoil (Fig. 3b'), infiltration could not be maintained

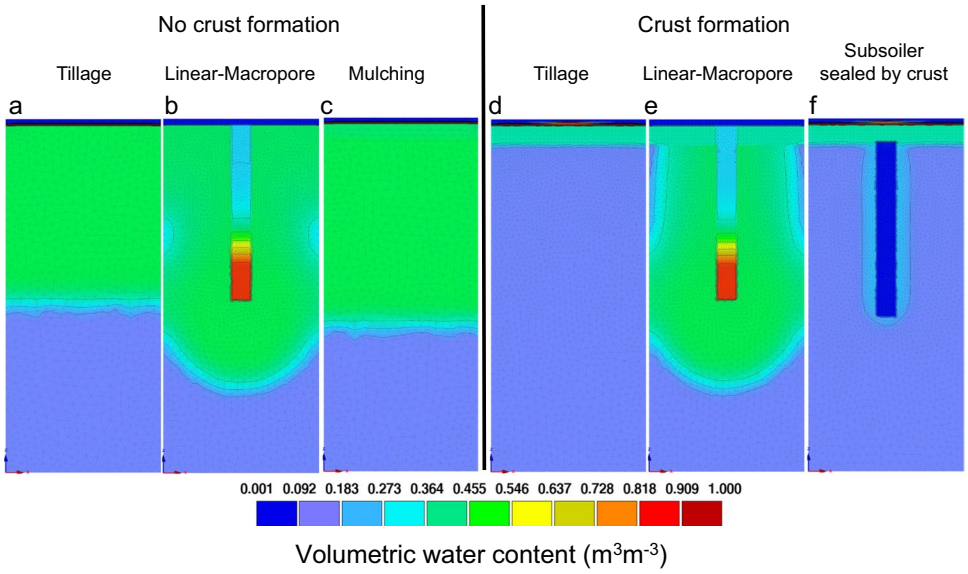

Fig. 4 2D-simulation results of macropore/no macropore with/without crust formation after one hour of rainfall

(Fig. 4f). Hence, the subsoilers developed in temperate regions are not likely to function under subtropical climates with dispersive soils in which surface crusts tend to form.

3.4 Soil Erosion

In general, the surface runoff volume after the second rainfall period was more extensive than that after the first (Fig. 5). As the soil was saturated at the beginning of the second rainfall period, we observed a large amount of surface water in the second rainfall period.

A substantial difference in soil erosion was observed among the treatments, with the tillage and subsoil treatments exhibiting large sediment loss, whereas the no-tillage-with-mulching and linear-macropore treatments exhibited less sediment loss. While the soil surface in the tillage and subsoil treatments was sealed by crusts and allowed sediment loss, the fissures in the linear-macropore treatment, as well as the surface covering provided by the mulch, effectively reduced sediment loss despite the presence of significant surface water. Thus, although surface runoff was not significantly different, soil erosion for the subsoiler and no-tillage-with-mulching treatments was significantly different (Kruskal–Wallis test, 0.05%).

4 Discussions

During 180–360 min after rainfall initiation, the surface flow was rapidly removed; therefore, we assumed that steady-state saturated flow was maintained. The saturated hydraulic conductivity was subsequently calculated in Fig. 6 using Eq. (1) based on the drainage water using Darcy's law.

$$J_s = -K_s \frac{H_{10} - H_0}{L_{10} - L_0} \tag{1}$$

where H_{10} and L_{10} are equal to 10 cm and H_0 and L_0 are equal to 0 cm.

Generally, the infiltration rates during the second rainfall period were lower than those during the first, as surface conditions deteriorated following the first rainfall period. Moreover, substantial differences in hydraulic conductivities were observed between the tillage/subsoil treatments and linear-macropore/no-tillage-with-mulching treatments; this trend did not change throughout the first or second rainfall periods.

Given that rainfall intensity of 20 mm h^{-1} (5.56×10^{-4} cm s^{-1}) was higher than the initial saturated hydraulic conductivity of all soils, surface flow occurred for all treatments, which is also possible during the storms that occur at the sugarcane field. However, infiltration intensities were significantly lower for the tillage and subsoiler treatments compared with the initial conductivity (Tukey–Kramer test, $p < 0.05$), indicating that surface crust in Fig. 3 might cause significant negative effects during the rainfall simulation. In contrast, the linear-macropore and no-tillage-with-mulching treatments alleviated these negative effects, as discussed later. During the two rainfall periods, the infiltration rates decreased from $10^{-3.43}$ to $10^{-4.23}$ (1/6.31) for the tillage, $10^{-4.45}$ (1/10.5) for the subsoil, $10^{-3.84}$ (1/2.57) for the linear-macropore, and $10^{-4.07}$ (1/4.36) for the mulching treatments.

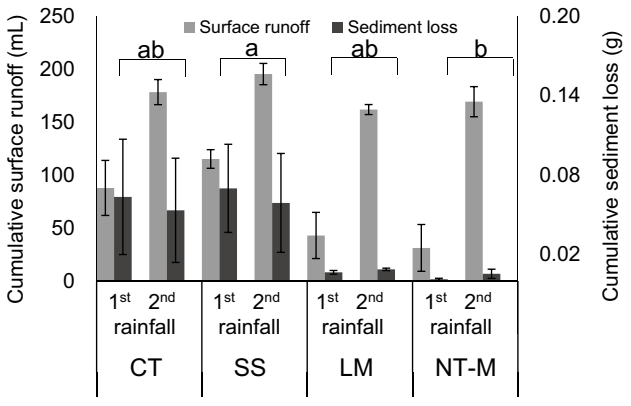

Fig. 5 Cumulative surface flow and sediment loss after the first and second rainfall periods. Error bars show standard errors. There was no significant differences in surface runoff, while sediment loss showed a significant difference between the subsoiler and no-tillage-with-mulching treatments (Kruskal–Wallis test, $p < 0.05$). CT: conventional tillage, SS: subsoiler, LM: linear-macropore, NT-M: no-tillage with mulching

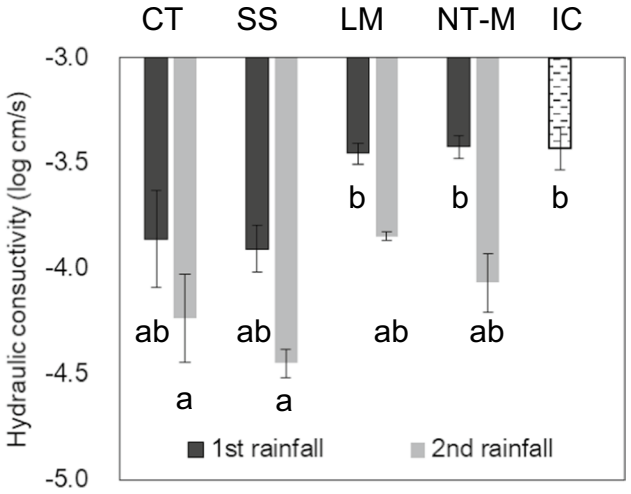

Fig. 6 Hydraulic conductivity calculated during the steady state flow period. The initial hydraulic conductivity was independently measured. Error bars show standard errors, while lower-case letter indicate significance based on Tukey–Kramer tests, $p < 0.05$. CT: conventional tillage, SS: subsoiler, LM: linear-macropore, NT-M: no-tillage with mulching, IC: initial conductivity

Next, we estimated the saturated hydraulic conductivity (K) of soil with a surface crust. Our observations indicated that the depth of the crust was only 0.5 cm, while the remaining 9.5 cm of the soil remained unchanged. We calculated the two-layer hydraulic conductivity, setting K_c at the crust layer (L_1: height 10–9.5 cm) to 2.0×10^{-6} cm s^{-1} (typical for clay soil) and K_o to 3.16×10^{-4} cm s^{-1} (core sample from the field, measured without the crust) for the remaining depth (L_2: height 9.5 to 0 cm). Darcy's equation for these two layers is represented by Eqs. (2) and (3):

$$J_c = -K_c \frac{H_{10} - H_{9.5}}{L_{10} - L_{9.5}} \tag{2}$$

$$J_o = -K_o \frac{H_{9.5} - H_0}{L_{9.5} - L_0} \tag{3}$$

Given that the flux, J, is the same through the two layers, we can assume that $J_c = J_o$. Note that L_{10}, $L_{9.5}$, and L_0 are 10, 9.5, and 0, respectively. H_{10} and H_0 can be assumed to be 10 and 0, and $H_{9.5}$ is unknown. By solving Eqs. (2) and (3), we obtained the resultant infiltration rate, $J_c = J_o$, to be 3.57×10^{-5} cm s^{-1}, which was 1/8.9 of the initial infiltration intensity. This calculated value corresponded well with the decrease in the measured infiltration rate of 1/6.31 for the tillage and 1/10.5 for the subsoiler treatments (Fig. 6). We postulate that the decrease in the infiltration rate was caused by crust formation at the soil surface, which already occurred after the first rainfall period. According to Onaga and Yoshinaga (1988), Kunigami Mahji soil is distributed over 50% of the entire Okinawa region and Ishigakijima Island. This soil shows a high rate of dispersion, i.e., the soil contains a small proportion of water-resistant aggregates that readily contribute to the formation of crusts, leading to surface flow. As the infiltration capacity deteriorated, the surface flow readily increased (Fig. 2). The subsoil treatment is assumed to increase the amount of water movement in the saturated soil layer (Miyazaki et al. 2005); however, despite the advantages of subsoil treatments in the temperate zone (He et al. 2021), within subtropical climates, such treatment can be expected to dissipate relatively quickly. On the other hand, even with crust formation at the soil surface of the artificial macropore treatment (Fig. 3c), the highest volume of drainage water was obtained (Fig. 2d). Hence, the application of fibrous material within the vertical gap successfully reinforced the structure of the linear artificial macropore and maintained its infiltration capacity, even after crust formation. In contrast, no crust was formed in the mulching treatment as the plant residues likely dampened the impact of the rain, thus preventing crust formation, which was corresponded well with Adekalu et al. (2007).

We calculated the water mass balance (Fig. 7a, b) after the first and second rainfall periods. The fraction of each component, as well as the surface flow, soil water content, and drainage, clearly showed water movements that reflected the aforementioned findings. Moreover, the 2D simulation results were converted to a mass balance (Fig. 7c) using an initial water content of 15% for no crust formation, while 40% were used for crust formation, as soils were saturated before initiating the second run. The calculated results with no crust formation (left three simulations in Fig. 7c) showed a similar trend as the experimental results in the first rainfall period (Fig. 7a), showing that the subsoiler treatment had almost the same effect as the tillage or no macropore treatments.

For crust formation (right three simulations in Fig. 7c), the tillage in Fig. 7c was similar to that in Fig. 7b, the second rainfall period. In addition, the subsoiler sealed by a crust (Fig. 7c) was similar to that in Fig. 7b, indicating dysfunctional subsoilers. The drainage in the macropore in Fig. 7c was more extensive than that in Fig. 7b; however, the results clearly showed that the artificial macropore structure, reinforced by fibrous material protruding above the soil surface, worked effectively for infiltration/drainage, even with crust formation. These simulation results confirm the experimental results in Fig. 7a, b.

The above surface flow or surface crust affected soil erosion. The 0.07 g of sediment lost per 120 mm of rainfall in the tillage and subsoil treatments (Fig. 5) was converted to 774 kg/ha/1,000 mm of rain, which was relatively close to the value reported for conventional tillage (1,200 kg/ha/1,000 mm) (Oka et al. 2022). Ishigakijima Island, Okinawa, Japan, has an annual rainfall of 2,106.8 mm (1981–2010, Japan Metrological Agency), and the surface soil has a carbon concentration of 1.73 g-C/100 g-soil (Table 1), with the resulting soil carbon loss estimated as 0.282 t-C ha^{-1} yr^{-1}. Such significant carbon loss would negate the 0.1–0.7 t-C ha^{-1} yr^{-1} carbon increase in cultivated fields within other regions (Hillel and Rosenzweig 2009). Therefore, the 0.01 g of soil lost per 120 mm of rainfall for the linear-macropore and no-tillage treatments (Fig. 6) can be considered a significant reduction relative to the other experimental cases. Moreover, the observed 1/7 reduction is reasonable, considering that Osawa et al. (2005) reported a reduction factor of 1/6.6 for a no-tillage treatment plot. Therefore, the linear-macropore treatment could be applied to sugarcane fields, along with the no-tillage treatment.

Finally, to evaluate these effects under actual rainfall, we conducted a field experiment, employing the four approaches (tillage, subsoil, linear-macropore, and

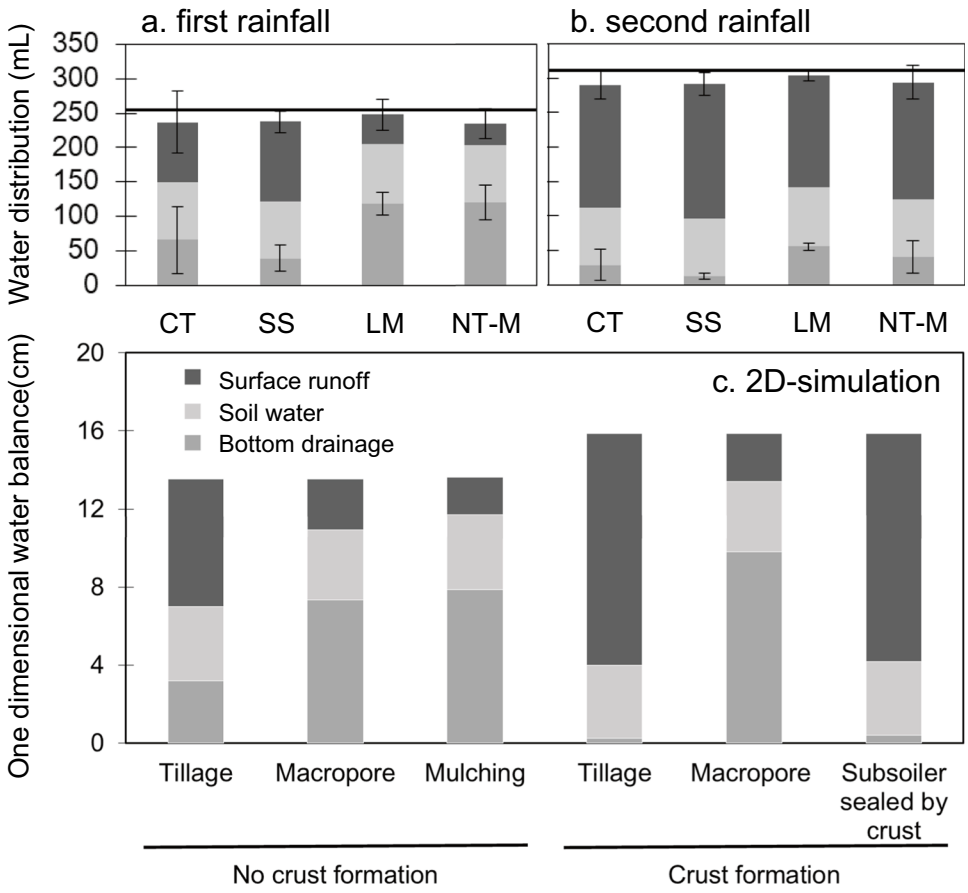

Fig. 7 Mass balance of water for experiments (**a**, **b**) and 2D-simulation (**c**). Error bars were added to surface runoff and drainage while the soil water showed saturated water content. The horizontal line denotes the sum of the initial and applied water volume. CT: conventional tillage, SS: subsoiler, LM: linear-macropore, NT-M: no-tillage with mulching

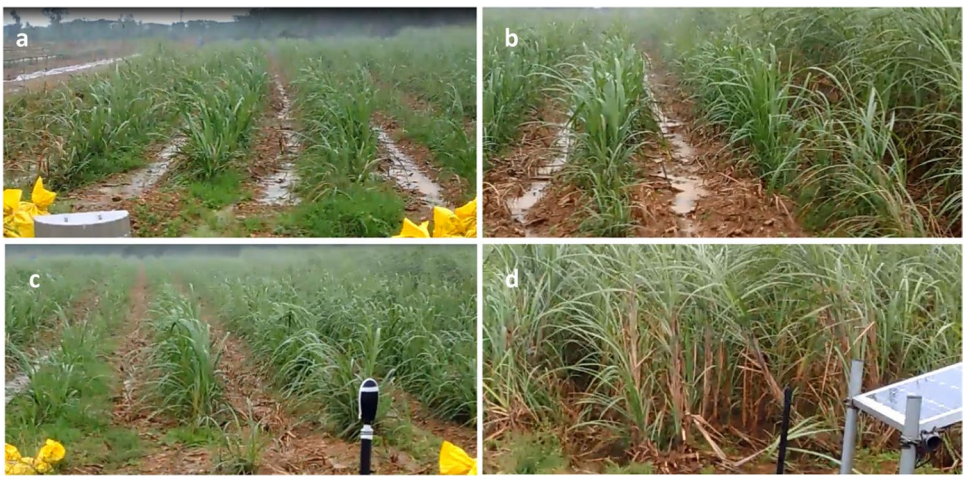

Fig. 8 Preliminary field application of the four treatments (**a**) tillage, (**b**) subsoiler, (**c**) linear-macropore, (**d**) no-tillage-with-mulching. Photos were captured on the same day at the same time

no-tillage-with-mulching treatments). Figure 8 presents images captured after 9.5 mm h^{-1} of rainfall at 11:30 am on December 27. Continuous rainfall occurred at 08, 09, 10, 11 a.m., and 12 p.m., with 2.0, 7.5, 3.5, 9.5, and 5.5 mm of precipitation, respectively. Water ponding was clearly observed in the tillage and subsoil plots; however, it was absent from the linear-macropore and no-tillage plots. Furthermore, less surface soil was lost from the linear-macropore and no-tillage plots compared with that from the tillage and subsoil treatment plots. While we are aware of the limitations of applying these experimental results to the field, these preliminary results provide sufficient theoretical evidence for potential field applications in sugarcane fields during the next season.

5 Conclusions

The following conclusions can be drawn from the application of the four different soil management strategies to mitigate the erosion of red soil.

Among the four treatments, the no-tillage and linear-macropore treatments successfully reduced surface runoff and sediment discharge. In the no-tillage treatment, the use of plant residues reduced the impact of raindrops, thus preventing crust formation. Moreover, the linear-macropore treatment improved infiltration by maintaining coarse structural gaps via the insertion of fibrous material. Therefore, linear macropores could also be suitable to counter red soil erosion.

In addition, given that the Okinawa region has abundant and high-intensity annual rainfall as well as soils that exhibit dispersive characteristics, even a coarse gap created by a subsoiler can become readily plugged by small particles, leading to crust formation. Hence, a coarse gap structure would not be effective, even if the impermeable layer was limited to the topsoil surface.

Finally, the soil carbon loss estimated from soil erosion was 0.282 t-C ha^{-1} yr^{-1}, which is sufficient to negate conservation management used in other fields. As the observed 1/7 reduction offers significant benefits, the linear-macropore treatment could be applied to sugarcane fields, along with no tillage.

This study aimed to evaluate measures to counteract soil erosion by the introduction of linear macropores. A set of comparatively small-scale experiments was conducted to understand the mechanism of erosion prevention. Superior results were obtained for the linear-macropore and no-tillage-with-mulching treatments in the laboratory experiments and 2D simulation analysis, as well as in a preliminary field application.

Acknowledgements The authors are grateful to the MSc and BSc students who have lent their assistance in the laboratory and preliminary field experiments since their inception in 2016. This work was partially supported by the Japan Society for the Promotion of Science NEXT program (GS021, 2011–2014), KAKENHI (B) (26292127, 2014–2016), KAKENHI (A) (17H01496, 2017–2020), KAKENHI (A) (21H04747, 2021–2024). This research was conducted as part of the ABRESO project, supported by the Japan Science and Technology Agency (JST) as part of the Belmont Forum.

Author Contributions Conceptualization: Yasushi Mori, Kazutoshi Osawa, and Akira Hoshikawa; Methodology: Eisei Morioka, Thanh Long Bui and Yasushi Mori; Formal analysis and investigation: Eisei Morioka, Thanh Long Bui and Yasushi Mori; Writing—original draft preparation: Eisei Morioka; Writing—review and editing: Yasushi Mori, Kazutoshi Osawa, and Akira Hoshikawa; Funding acquisition, Resources and Supervision: Yasushi Mori.

Funding Open access funding provided by Okayama University. This work was partially supported by the Japan Society for the Promotion of Science NEXT program (GS021, 2011–2014), KAKENHI (B) (26292127, 2014–2016), KAKENHI (A) (17H01496, 2017–2020), KAKENHI (A) (21H04747, 2021–2024). This research was conducted as part of the ABRESO project, supported by the Japan Science and Technology Agency (JST) as part of the Belmont Forum.

Data Availability Data will be made available on request.

Declarations

Competing Interests The authors declare that they have no competing interests.

References

Adekalu KO, Olorunfemi IA, Osunbitan JA (2007) Grass mulching effect on infiltration, surface runoff and soil loss of three agricultural soils in Nigeria. Biores Technol 98:912–917

FAO, ISRIC, ISSS (2006) World Reference Base for Soil Resources 2006, A framework for international classification, correlation and communication. FAO World Soil Resour Rep 103:1–128

Gjettermann B, Hansen HCB, Jensen HE, Hansen S (2004) Transport of phosphate through artificial macropores during film and pulse flow. J Environ Qual 33:2263–2271. https://doi.org/10.2134/jeq2004.2263

Guillaume T, Damris M, Kuzyakov Y (2015) Losses of soil carbon by converting tropical forest to plantations: Erosion and decomposition estimated by δ13C. Glob Chang Biol 21:3548–3560. https://doi.org/10.1111/gcb.12907

He D, Lu C, Tong Z, Zhong G, Ma X (2021) Research progress of minimal tillage method and machine in China. AgriEngineering 3:633–647. https://doi.org/10.3390/agriengineering3030041

Hillel D, Rosenzweig C (2009) Soil carbon and climate change. CSA News 54:4–11

Hudson NW (1981) Soil conservation, 2nd edn. Batsford, London

Ikeda S, Kan K (2014) Chapter 6. Red soil runoff and conservation of coral reefs, reproduction. In: Research Center for Sustainable Communities (kokudobunka kenkyujo) (ed) Control of sediment nutrient dynamics for environmental conservation and regeneration. Kindai kagaku sha Co., Ltd., Tokyo, pp 121–167

Japan Meteorological Agency (2023) Tables of monthly climate statistics.https://www.data.jma.go.jp/obd/stats/data/en/smp/index.html. Accessed 28 June 2023

Kanazawa S (1995) The no-tillage cropping system as the agriculture for sustaining and environmental preservation - crop yields and soil characteristics. Soil Sci Plant Nutr 66:286–297

Komissarov MA, Klik A (2020) The impact of no-till, conservation, and conventional tillage systems on erosion and soil properties in lower Austria. Eurasian Soil Sc 53:503–511. https://doi.org/10.1134/S1064229320040079

Lal R (2001) Soil degradation by erosion. Land Degrad Dev 12:519–539. https://doi.org/10.1002/ldr.472

Lamy E, Lassabatère L, Bechet B, Andrieu H (2009) Modeling the influence of an artificial macropore in sandy columns on flow and solute transfer. J Hydrol 376:392–402. https://doi.org/10.1016/j.jhydrol.2009.07.048

Miura T, Niswati A, Swibawa IG et al (2016) Shifts in the composition and potential functions of soil microbial communities responding to a no-tillage practice and bagasse mulching on a sugarcane plantation. Biol Fertil Soils 52:307–322. https://doi.org/10.1007/s00374-015-1077-1

Miyazaki T, Hasegawa S, Kasubuchi T (2005) Soil Physics. 121, Asakura Publishing Co., Ltd., Tokyo, Japan

Mori Y, Higashi N (2009) Controlling solute transport processes in soils by using dual-porosity characteristics of natural soils. Colloids Surf A Physicochem Eng Asp 347:121–127. https://doi.org/10.1016/j.colsurfa.2009.02.009

Mori Y, Hirai Y (2014) Effective vertical solute transport in soils by artificial macropore system. J Hazard Toxic Radioact Waste 18:1–7. https://doi.org/10.1061/(ASCE)HZ.2153-5515.0000192

Mori Y, Iwama K, Maruyama T, Mitsuno T (1999a) Discriminating the influence of soil texture and management-induced changes in macropore flow using soft X-rays. Soil Sci 164:467–482

Mori Y, Maruyama T, Mitsuno T (1999b) Soft X-ray radiography of drainage patterns of structured soils. Soil Sci Soc Am J 63:733–740. https://doi.org/10.2136/sssaj1999.634733x

Mori Y, Suetsugu A, Matsumoto Y, Fujihara A, Suyama K (2013) Enhancing bioremediation of oil-contaminated soils by controlling nutrient dispersion using dual characteristics of soil pore structure. Ecol Eng 51:237–243. https://doi.org/10.1016/j.ecoleng.2012.12.009

Mori Y, Fujihara A, Yamagishi K (2014) Installing artificial macropores in degraded soils to enhance vertical infiltration and increase soil carbon content. Prog Earth Planet Sci 1:30. https://doi.org/10.1186/s40645-014-0030-5

Morin J, Benyamini Y, Michaeli A (1981) The effect of raindrop impact on the dynamics of soil surface crusting and water movement in the profile. J Hydrol 52:321–335

Moss AJ (1991) Rain impact soil crust. I. Formation on a granite derived soil. Soil Res 29:271–289. https://doi.org/10.1071/SR9910271

Mualem Y (1976) A new model for predicting the hydraulic conductivity of unsaturated porous media. Water Resourc Res 12:513–522. https://doi.org/10.1029/WR012i003p00513

Nakasone K, Higa E, Mitsumoto H, Omija T (1998) Estimation of soil loss in Okinawa prefecture (II). Ann Rep Okinawa Prefectural Inst Health Environ 32:67–72

Noda K, Osawa K, Ikeda S, Ozawa K (2009) Evaluating on agricultural practices for effective sediment yield reduction on sugarcane fields, Okinawa. Trans JSIDRE 260:47–56. https://doi.org/10.11408/jsidre.77.153

Oka K, Bui TL, Mori Y, Osawa K, Hoshikawa A (2022) Artificial macropore installation and no-tillage practice in subtropical sugarcane field to conserve water and organic matter in soils. J Jpn Soc Soil Phys 150:93–103. https://doi.org/10.34467/jssoilphysics.150.0_93

Onaga K, Gibo S (1984) Special soil in Japan (Part 11 - Final lecture) - Special soil in Okinawa (Mahji and Jahgaru). Jour JSIDRE 52:49–56. https://doi.org/10.11408/jjsidre1965.52.6_517

Onaga K, Yoshinaga A (1988) Physical properties of major Okinawan upland soils. J Jpn Soc Soil Phys 58:17–29. https://doi.org/10.34467/jssoilphysics.58.0_17

Osawa K, Yamaguchi S, Ikeda S, Takamuku K (2005) Field observation of sediment runoff reduction methods on farmland. Proc Hydraul Eng 49:1099–1104. https://doi.org/10.2208/prohe.49.1099

Prefecture O (2014) Sugarcane cultivation guide. Cultivation Manag 3:8–19

Richard G, Cousin I, Sillon JF, Bruand A, Guérif J (2001) Effect of compaction on the porosity of a silty soil: influence on unsaturated hydraulic properties. Eur J Soil Sci 52:49–58. https://doi.org/10.1046/j.1365-2389.2001.00357.x

Simunek J, Sejna K, van Genuchten M Th (2007) The HYDRUS software package for simulating two- and three-dimensional movement of water, heat, and multiple solutes in variably-saturated media, User Manual, Ver. 1.0. PC-Progress, Prague, Czech Republic

Six J, Paustian K, Elliott ET, Combrink C (2000) Soil structure and organic matter I. Distribution of aggregate-size classes and aggregate-associated carbon. Soil Sci Soc Am J 64:681–689. https://doi.org/10.2136/sssaj2000.642681x

Tebrügge F, Düring RA (1999) Reducing tillage intensity - a review of results from a long term study in Germany. Soil Tillage Res 53:15–28. https://doi.org/10.1016/S0167-1987(99)00073-2

van Genuchten MTH (1980) A closed-form equation for predicting the hydraulic conductivity of unsaturated soils. Soil Sci Soc Am J 44:892–898. https://doi.org/10.2136/sssaj1980.03615995004400050002x

Wang Z, Hoffmann T, Six J, Kaplan JO, Govers G, Doetterl S, Van Oost K (2017) Human-induced erosion has offset one-third of carbon emissions from land cover change. Nature Clim Change 7:345–349. https://doi.org/10.1038/nclimate3263

Yagioka A, Komatsuzaki M, Kaneko N, Ueno H (2015) Effect of no-tillage with weed cover mulching versus conventional tillage on global warming potential and nitrate leaching. Agric Ecosyst Environ 200:42–53. https://doi.org/10.1016/j.agee.2014.09.011

Zhang Y, Zhang R, Zhang B, Xi X (2021) Artificial macropores with sandy fillings enhance desalinization and increase plant biomass in two contrasting salt-affected soils. Appl Sci 11:3037. https://doi.org/10.3390/app11073037